From default-mode to action-mode: biphasic network reconfiguration with meditation in schizophrenia

Qing Wang[1,2*], Lizhao Du[1,3], Jialing Sheng[4], Qiao Wang[5], Yuan Shi[1], Ting Xue[1], Zhong Sun[4], Yingying Tang[1,2], Donghong Cui[1,6*]

1. Shanghai Key Laboratory of Psychotic Disorders, Brain Health Institute, National Center for Mental Disorders, Shanghai Mental Health Center, School of Medicine, Shanghai Jiao Tong University, Shanghai, 200030, China.

2. NeuroImaging Core, Shanghai Mental Health Center, School of Medicine, Shanghai Jiao Tong University, 600 S. Wanping Rd., Shanghai, 200030, China.

3. Shanghai Med-X Engineering Research Center, School of Biomedical Engineering, Shanghai Jiao Tong University, Shanghai, China

4. The First Minzheng Mental Health Center, No. 9999 Zhongchun Rd., Minhang, Shanghai, 201105, China.

5. Department of Public Health, Brody School of Medicine, East Carolina University, 610 Moye Blvd, Mailstop 660, Greenville, NC 27834, U.S.A.

6. Brain Science and Technology Research Center, Shanghai Jiao Tong University, Shanghai, China.

*To whom correspondence should be addressed.

Contact: vincent.w.qing@gmail.com, manyucc@126.com

Author notes:

Qing Wang: https://orcid.org/0000-0002-6843-5516

Lizhao Du: https://orcid.org/0000-0003-4664-0938

Qiao Wang: https://orcid.org/0000-0002-3570-9496

Ting Xue: https://orcid.org/0000-0002-3650-6308

Yingying Tang: https://orcid.org/0000-0002-4705-3682

Abstract

Whether and how meditation benefits severe psychosis over clinically meaningful timescales remains unclear. We embedded longitudinal neuroimaging in an eight-month, parallel-group randomized clinical trial (ChiCTR1800014913) of male inpatients (n=64) with schizophrenia receiving daily clinician-guided meditation plus rehabilitation versus rehabilitation alone. Meditation improved the symptoms by 11.8% at 3 months and 20.8% at 8 months (average treatment effects of PANSS decrease rates) and increase the cognition (RBANS) by 7.6% at 3 months that plateaued. Early cognition improvement predicts but not mediates later symptom relief. Resting-state fMRI revealed a biphasic pattern related to symptom improvement: baseline default-mode–cerebellar complexity predicted 3-month benefit, whereas 3-month action-mode/sensorimotor–executive complexity predicted 8-month gains, which was mirrored by functional connectivity prediction models. These findings support a biphasic network reconfiguration model for meditation: early default-mode–cerebellar involvement followed by later action-mode engagement, and provide phase-specific, information-based markers for personalized meditation in schizophrenia.

Introduction

Meditation, encompassing focused attention to open monitoring and compassion practices, yields small to moderate improvements in stress, mood and wellbeing with good acceptability across settings[1–3]. The field has shifted from "*does it work*?" toward "*for whom, when, and through which neural processes"*, alongside more precise reporting of dose and componentry[4,5]

Beyond general mental-health gains, randomized and assessor-blinded trials in severe brain disorders suggest clinically meaningful but condition-dependent benefits[3]. Examples include Parkinson's disease (mood and quality-of-life gains without motor compromise)[6,7], chronic pain (mindfulness-based stress reduction comparable to cognitive behavioral therapy at 26 weeks)[8], migraine (disability improved without reducing attack frequency)[9], prevention of depressive relapse[10] and post-traumatic stress disorder[11]. In schizophrenia, one of the most severe mental disorders, meta-analyses indicated small to moderate improvements in total and negative symptoms[1,12]. A recent intensive, clinician-guided program produced robust PANSS (Positive and Negative Syndrome Scale) reductions and better quality of life versus rehabilitation alone[13]. Yet, most trials are typically short, privilege single primary outcome, and seldom model response heterogeneity or cross-domain coupling of benefits.

Converging neuroimaging studies indicate that meditation reshapes large-scale brain network organizations: meditation practice tends to dampen activities in self-referential systems and strengthen executive and frontoparietal coupling at rest, with training-dependent shifts in community structure and network allegiance[14–18]. Beyond functional connectivity, temporal complexity of the BOLD signal (captured by scale-free dynamics and entropy-based irregularity) indexes adaptive capacity, increases with practice, and distinguishes clinical populations, including schizophrenia[19–21]. Recent multivariate work in experimentally evoked pain further shows that meditation reduces pain via neural signatures that are distinct from placebo, reinforcing mechanism-specific pathways beyond expectancy[22]. For psychiatric conditions, meditation-imaging findings broadly converge on attenuated default-mode dominance and enhanced executive control, with early randomized trials showing resting-state strengthening of executive networks after training[14–16]. These meditation effects are naturally organized along an axis from internally oriented, self-referential mentation to externally oriented, action-focused control. Foundational parcellations and cerebellar maps outline tightly coupled cortico–cerebellar

topographies and gradients from sensorimotor to transmodal territories, providing the large-scale canvas for brain functional reconfiguration[23–25]. Contemporary syntheses refine the default mode network (DMN)[26] as supporting autobiographical memory, self-reference, and narrative construction, and propose an action-mode network (AMN)[27,28] that sustains goals, orients attention outward, and updates actions; cerebro–cerebellar loops plausibly calibrate both modes via predictive control[29]. Yet schizophrenia remains under-imaged: most studies are small and underpowered, cross-sectional or short-term, rarely randomized; cerebellar coupling is seldom modeled explicitly; and temporal-complexity metrics are infrequently deployed despite their sensitivity to both training and disease[19,20]. Across the field, longitudinal RCT with neuroimaging is scarce, early versus late stage benefits is rarely modeled, and conclusions can diverge when using complexity versus functional connectivity measures. These gaps call for randomized, longitudinal designs that pair clinically interpretable endpoints with information-rich biomarkers that can track plasticity on actionable timescales.

Here, we embedded longitudinal neuroimaging within an eight-month, parallel-group randomized clinical trial of inpatients with schizophrenia comparing daily clinician-guided meditation plus rehabilitation with rehabilitation alone (ChiCTR1800014913)[13] We prespecified symptom (PANSS) and cognition (measured by Repeatable Battery for the Assessment of Neuropsychological Status, RBANS) endpoints and estimated time-specific average treatment effects with linear mixed-effects models. To probe temporal ordering, we tested whether early cognitive changes precede later symptom change using a cross-lagged panel model. To address treatment-response heterogeneity, we fit latent-class linear mixed models for PANSS reduction rates to identify subgroups with distinct longitudinal trajectories[30], and identified the most predictive baseline characteristics for high-responders.

To generate mechanistic insights, we acquired resting-state fMRI at baseline, 3 months and 8 months. Using group canonical ICA (Independent Component Analysis)[31], we derived two data-driven components aligned with the clinical improvement: a default-mode–cerebellar integrative component (DMN–CIC) and an action-mode–sensorimotor–executive component (AMN–SEC). For each component, we quantified temporal complexity (sample entropy; Hurst exponent) and formed a composite complexity index as an information-based readout of neural flexibility. We related these measures to PANSS decrease rates for meditation and rehabilitation groups and further asked whether these two components played different roles in early and late stages. On the other hand, we also asked whether baseline resting-state functional connectivity (rsFC) and early rsFC changes (0–3 months) can predicted 3- and 8-month clinical benefits using cross-validated elastic-net models with permutation-based importance[32]. These two families of brain functional measures showed consistent predictive roles for DMN-CIC and AMN-SEC, providing longitudinal, information-rich biomarkers aligned to clinically meaningful timescales, with a concurrent rehabilitation arm for specificity.

Together, this design tests a biphasic reconfiguration hypothesis: early attenuation of DMN–CIC integration followed by later recalibration of AMN–SEC coupling, and links component dynamics to who benefits, when, and in which domains. By estimating time-specific treatment effects, modeling response heterogeneity, and coupling outcomes to composite neural complexity and connectivity predictors, we aim to bridge the evidentiary gap between clinical benefit and large-scale brain functional reorganization in a form that is actionable for personalized meditation.

Results

Meditation produces progressive symptom improvement and plateauing cognitive gains

The experimental procedures were demonstrated in Fig. 1a. Linear mixed-effects models (LMM) indicated a time-increasing treatment benefit on PANSS decrease rate (PDR) and an early, modest cognitive gain that plateaued. As illustrated in Fig. 1b, the average treatment effect (ATE) for PDR was 11.807% after 3 months (95% CI: 9.323% – 14.292%, $p<0.001$) and 20.772% after 8 months (95% CI: 15.989% – 25.554%, $p < 0.001$). Cognitive improvement (RBANS increase rate, RIR) was modest and front-loaded: 7.618% after 3 months (95% CI: 2.413% – 12.824%, $p = 0.004$) and not significant after 8 months (5.518%, 95% CI: −2.053% – 13.090%, $p = 0.153$) (Fig. 1c). Baseline chlorpromazine equivalents (CPZ) dose, PANSS, RBANS, and FFMQ did not robustly moderate these effects. (Tab. S3-S12 in supplementary materials).

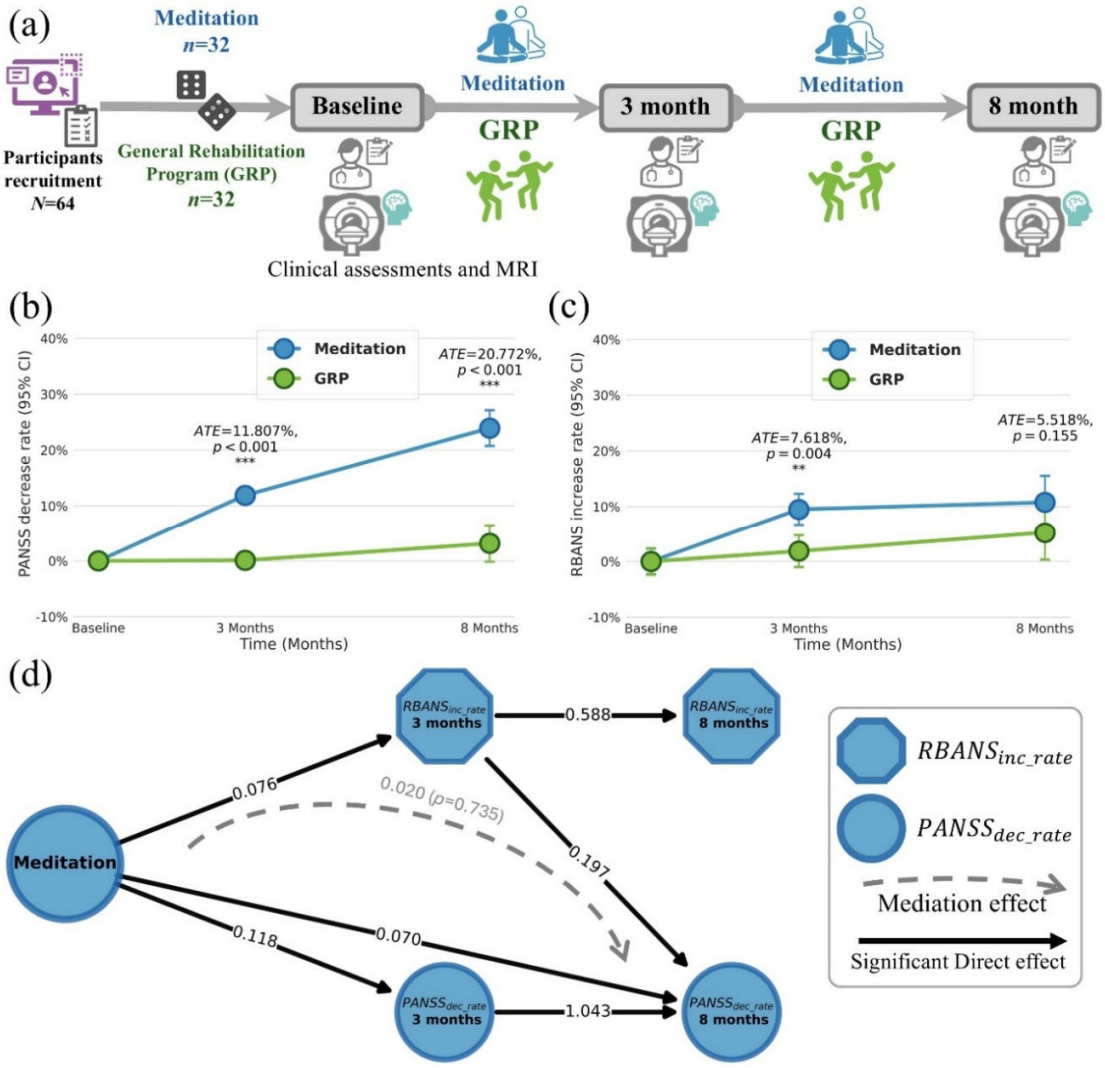

Figure 1. Experimental design, the treatment effects of meditation and their interplay. (a) Overview of the randomized controlled trial (RCT); (b) Average treatment effect (ATE) of meditation on PANSS decrease rate (PDR) over time; (c) ATE of meditation on RBANS increase rate (RIR) over time; (d) 3-month RIR predicts but not mediates the treatment effect of 8-month PDR. (PANSS: Positive and Negative Syndrome Scale; RBANS: Repeatable Battery for the Assessment of Neuropsychological Status)

Early cognitive gains forecast but not mediate later symptom relief

A cross-lagged panel model (CLPM) confirmed the direct treatment effect on PDR at 3-month: 0.118 ($p < 0.001$). The direct treatment effect at 8-month was 0.070 ($p = 0.036$), the indirect effect via 3-month PDR was 0.123, giving a total effect of 0.193. The treatment effect of 3-month RIR was 0.076 ($p = 0.011$), while no direct significant treatment effect was identified for 8-month RIR. The autoregression paths were significant for both PDR and RIR. (PDR: 1.043, $p < 0.001$; RIR: 0.588, $p < 0.001$). Crucially, 3-month RIR predicted 8-month PDR (0.197, p=0.017), while 3-month PDR did not predict 8-month RIR (0.020, p=0.946). A 10,000-bootstrap test showed a small, non-significant indirect effect of treatment on 8-month PDR via 3-month RIR (0.020, 95% CI: −0.0004 – 0.0479, $p = 0.7349$). Baseline CPZ was included as a covariate. In sum, early cognitive gains forecast symptom relief later but do not mediate it. The full path model and results are detailed in supplementary materials Tab. S14 and Fig. S2.

Meditation elicits heterogeneous clinical trajectories across individuals

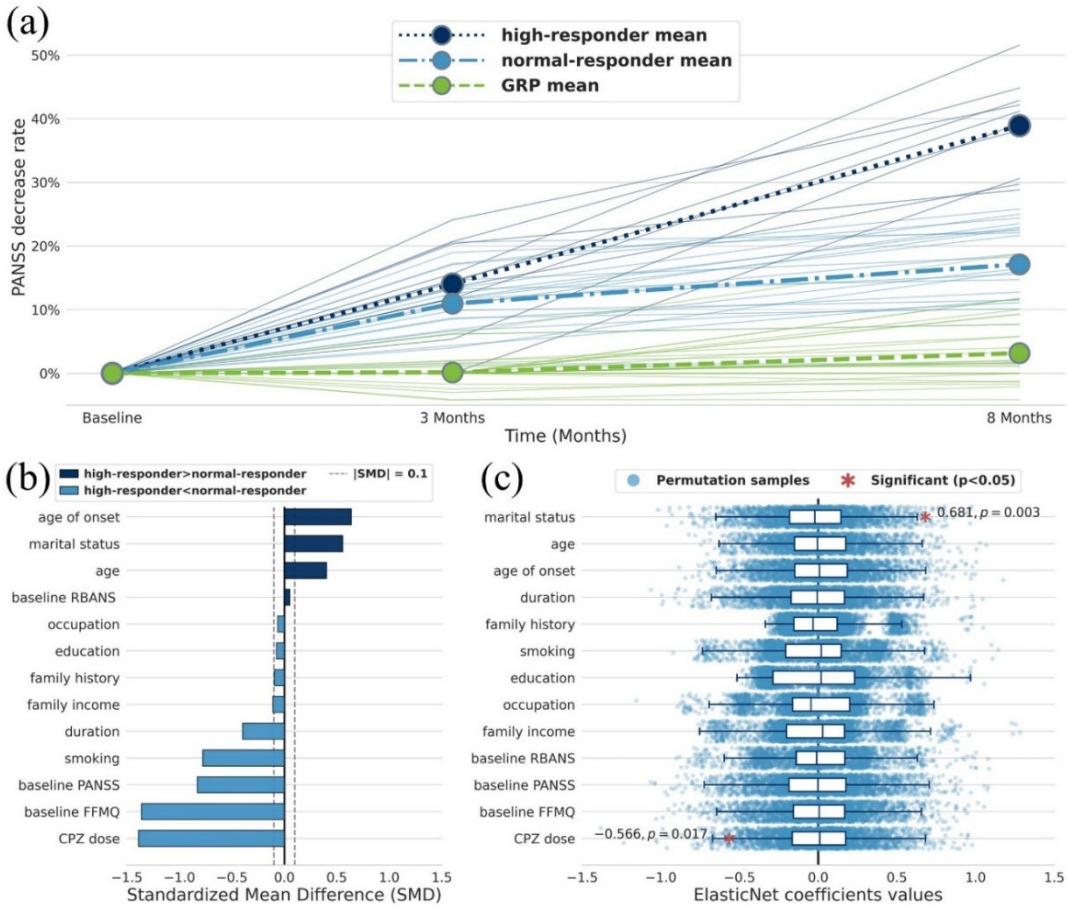

Figure 2. Heterogeneous response trajectories of meditation and the related predictors. (a) Clinical response trajectories for high-responders, normal-responders, and the general rehabilitation group (GRP); (b) Standardized mean differences (SMDs) between high-responders and normal-responders across baseline characteristics; (c) Permutation distribution (n=10,000) of elastic net logistic regression for high- and normal-responders; marital status and CPZ dosage were identified as significant predictors for high-responders.

Latent-class linear mixed models revealed heterogeneous clinical trajectories within the meditation arm, comprising a high-responder subgroup (n=10) and a normal-responder subgroup (n=22). As demonstrated in Fig. 2a, the mean PDR trajectories were similar through the first 3 months for both subgroups; thereafter, the high-responders continued to accrue gains, while the normal-responders decelerated, showing smaller subsequent clinical benefits (both outperforming the rehabilitation-only arm; n=31; one dropout). Baseline profiles (standardized mean differences in Fig. 2b) suggested that high-responders were more often married and on lower CPZ dose among other differences. In elastic net logistic models with permutation inference (Fig. 2c), marital status (β = 0.681, p = 0.003) and lower CPZ (β = −0.566, p = 0.017) remained robust correlates with high-responders. These findings underscore the treatment heterogeneity and nominate baseline social support and medication burden as pragmatic markers for prospective testing.

Biphasic components reconfigurations characterize the clinical gain

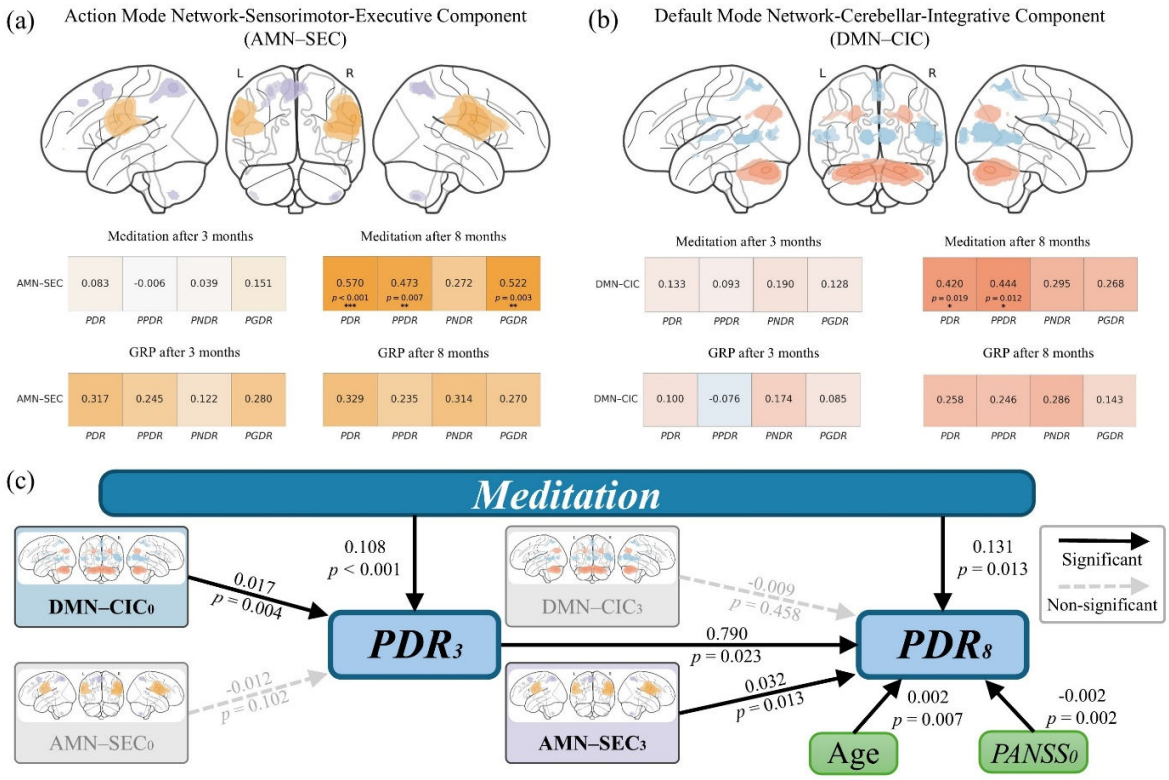

Figure 3 The action mode network–sensorimotor–executive component (AMN–SEC), the default mode network–cerebellar integrative component (DMN–CIC) and their correlations with clinical improvements over time. (a) The AMN–SEC and its correlations with clinical improvements across groups over time; (b) The DMN–CIC and its correlations with clinical improvements across groups over time; (c) The two-wave biphasic components contribution model for clinical improvements. (PDR: PANSS decrease rate; PPDR: PANSS Positive score Decrease Rate; PNDR: PANSS Negative score Decrease Rate; PGDR: PANSS General score Decrease Rate)

Group canICA identified two components (Fig. 3a-b): an action mode network–sensorimotor–executive component (AMN–SEC) and a default mode network–cerebellar integrative component (DMN–CIC). Permutation-validated screens linked three complexity metrics to better clinical outcome: higher AMN–SEC sample entropy (SampEn), lower AMN–SEC Hurst Exponent (HE), and lower DMN–CIC HE, and these metrics have been further validated by SHAP value[33] (Fig.

S3 in supplementary materials). AMN–SEC comprised bilateral precentral gyri, superior, middle, and inferior frontal regions, Rolandic opercula, insulae, mid-cingulate, sensorimotor cortices, supramarginal gyri, precuneus, superior temporal gyri, and inferior motor cerebellar lobules (VIIb–VIII). It is involved in cognitive control, sensorimotor integration, and goal-directed behaviors[27,28]. DMN–CIC included posterior cingulate, calcarine and lingual regions, superior and middle occipital areas, superior parietal cortex, precunei, middle temporal gyrus, extensive posterolateral cerebellar hemispheres (Crus I/II, lobules VI–VIII), and vermal lobules IV–IX. DMN–CIC is involved in high-level integrative processes: self-referential ideation, sensory-cognitive binding, and internal modeling[26].

Correlations between components complexities and symptom improvements exhibited distinct patterns for meditation and control arms (Fig. 3a–b). At 3-month for the meditation arm, neither component's CCI (Composed Complexity Index) showed a material association with concurrent symptom improvement (total PDR or domain-specific PPDR/PNDR/PGDR): effect sizes were small and non-significant (e.g., $r_{(CCI_3^{DMN-CIC}, PDR_3)} = 0.131,\ p = 0.467$, $r_{(CCI_3^{AMN-SEC}, PDR_3)} = 0.083,\ p = 0.650$; all domain correlations $|r| \leq 0.190, p \geq 0.310$). After 8 months of meditation, associations strengthened and became significant for both AMN–SEC and DMN-CIC: AMN–SEC CCI correlated with PDR ($r = 0.570, p < 0.001$), PPDR ($r = 0.473, p = 0.007$), and PGDR ($r = 0.522, p = 0.003$); the PNDR correlation was smaller and not significant ($r = 0.272, p = 0.146$). DMN–CIC CCI also related to total PDR ($r = 0.420, p = 0.019$) and PPDR ($r = 0.444, p = 0.012$), with weaker and non-significant associations for PNDR ($r = 0.295, p = 0.114$) and PGDR ($r = 0.268, p = 0.144$). Full correlation matrices and exact p-values were provided in supplementary materials. For the control arm, correlations were attenuated at both timepoints with no large or significant associations (largest effects at 8 months for AMN-SEC: $r_{(CCI_8,\ PDR_8)} = 0.329,\ p = 0.076$; for DMN-CIC: $r_{(CCI_8,\ PNDR_8)} = 0.286,\ p = 0.132$).

To further probe the cross-sectional contributions of these two components, we fit a two-wave lagged SEM model focused on PDR_3 and PDR_8. The model fit was good with scaled $\chi^2(37) = 39.321, p = 0.366$, the variances explained for PDR_3 and PDR_8 are 71.5% and 71.6% respectively. Baseline DMN–CIC CCI predicted greater 3-month PDR ($\beta = 0.017, 95\%CI: 0.005 - 0.029$, $p = 0.004$), whereas 3-month AMN–SEC CCI predicted 8-month PDR after accounting for PDR_3 ($\beta = 0.032, 95\%CI: 0.007 - 0.057$, $p = 0.013$).However, the reciprocal effects were not significant. Planned within-phase contrasts favored DMN–CIC in the early window and AMN–SEC in the late window (Wald test $p = 0.009$ and $p = 0.047$ respectively).

Taken together, the CCI correlations (small at 3 months; larger and significant by 8 months, especially for AMN–SEC) and the time-ordered SEM support a biphasic contribution model for meditation in which early improvement aligns with DMN–CIC at baseline and later gains align with AMN–SEC at mid-treatment—a pattern that was not evident under rehabilitation alone.

Functional connectivity predicts short- and long-term clinical responses under meditation

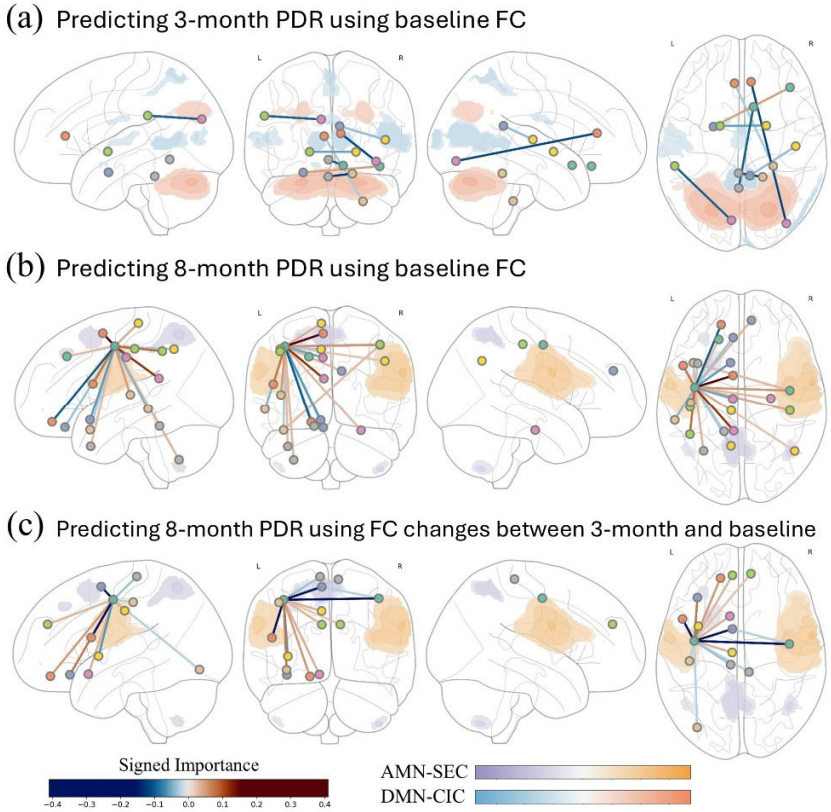

FC pairs	Signed Importance	Std.
Cerebellum_4_5_R - Vermis_1_2	-0.119	0.035
Cingulum_Ant_R - Occipital_Inf_R	-0.110	0.033
Olfactory_R - Vermis_4_5	-0.091	0.028
Cuneus_L - SupraMarginal_L	-0.091	0.030
Pallidum_L - Pallidum_R	-0.054	0.018

FC pairs	Signed Importance	Std.
Precentral_L - Supp_Motor_Area_L	0.154	0.028
Precentral_L - Cingulum_Post_L	0.110	0.020
Precentral_L - Frontal_Sup_Orb_L	-0.095	0.018
Precentral_L - Parietal_Inf_L	0.078	0.014
Precentral_L - Frontal_Inf_Oper_L	0.069	0.013
Precentral_L - Olfactory_L	-0.058	0.011
Precentral_L - Precentral_R	0.052	0.010
Precentral_L - Cingulum_Mid_L	-0.052	0.009

FC pairs	Signed Importance	Std.
Precentral_L - Supp_Motor_Area_L	-0.371	0.067
Precentral_L - Frontal_Inf_Oper_L	-0.322	0.059
Precentral_L - Precentral_R	-0.253	0.046
Precentral_L - Frontal_Inf_Orb_L	0.070	0.013
Precentral_L - Insula_L	-0.062	0.011

(Importance>0.05)

Figure 4 Predicting PANSS decrease rate (PDR) using Functional Connectivity (FC) for the meditation group. (a) Prediction of 3-month PDR using baseline FC features, with the default mode network–cerebellar integrative component (DMN–CIC) as the background brain map; FCs with importance ≥0.05 are summarized in the left panel; (b) Prediction of 8-month PDR using baseline FC features, with the action mode network–sensorimotor–executive component (AMN–SEC) as the background brain map; FCs with importance ≥0.05 are summarized in the left panel; (c) Prediction of 8-month PDR using FC changes over the first 3 months, with AMN–SEC as the background brain map; FCs with importance ≥0.05 are summarized in the left panel. (FCs with importance ≥0.02 are visualized in the brain maps.)

Elastic net regression with permutation importance was used to identify robust functional connectivity (FC) features that predicted clinical gains (PDR) in 3 tasks (Fig. 4). Meditation group results revealed robust predictive utility for all tasks. For short-term response (PDR at 3 months), stronger baseline DMN–CIC couplings were associated with less improvement—most notably *Cerebellum_4-5_R – Vermis_1-2* (–0.119), with similar trends for *Cingulum_Ant_R – Occipital_Inf_R*, *Olfactory_R – Vermis_4-5*, *Cuneus_L – Supramarginal_L*, and *Pallidum_L – Pallidum_R*. For long-term response (PDR at 8 months), baseline AMN–SEC couplings, and especially early changes in *precentral – motor/executive* FC (3-0 months), showed largest predictive power; *Precentral_L – SMA_L* was the strongest marker (baseline importance 0.154; early-change importance 0.371). The left precentral gyrus emerged as a pivotal hub across predictive edges. In the control arm, FC features showed minimal predictive power (largest importance 0.023). These FC results converge with the previous CCI–SEM findings, mirroring the biphasic contribution model: DMN–CIC characteristics in early benefit and AMN–SEC recalibration in later benefit.

Discussions

Daily clinician-guided meditation plus rehabilitation produced progressive symptom improvement across eight months, with front-loaded cognitive gains that plateaued and heterogeneous response across patients. Longitudinal imaging indicated a biphasic brain functional shift: early improvement tracked by default-mode–cerebellar dynamics, whereas later gains aligned with action-mode/sensorimotor–executive dynamics, with precentral–SMA connectivity emerging as a longer-term marker. This pattern is consistent with a mode-based axis of large-scale brain functional networks, in which internally oriented DMN activity yields to externally oriented action-mode control as goal-directed behaviors consolidates[26–28].

Since meditation practice is heterogeneous across applications, varying by dose, component mix and delivery, a daily and clinician-guided, skills-scaffolded program is clinically friendly (fits ward routines) and safety-oriented, while scalable self-administered formats remain attractive for step-care or maintenance[2]. Our results complement evidence that self-administered mindfulness reduces stress at scale in randomized settings and extend schizophrenia-focused meta-analytic conclusions by adding time-resolved neural readouts inside a randomized design[3]. Future work are still needed to benchmark formats against phase-specific targets.

Mechanistically, symptom and cognition improved on partly independent tracks, early cognitive change forecast later symptoms but did not mediate them, suggesting distinct pathways. Among them, the symptom improvement can be captured by the composite complexity index (CCI) and connectivity patterns in a biphasic fashion. The posterior cerebellum's repeated involvement is notable: cerebello-thalamo-cortical circuits support predictive/feedforward control and calibrate cortical dynamics during skill acquisition and switching, providing a substrate for the late action-mode engagement we observed[29].

From a personalized meditation perspective, these imaging markers can inform who benefits, when, and how to deliver care. Baseline DMN–cerebellar features (CCI/FC) nominate patients who likely to achieve early gains; 0 to 3-month changes in AMN (especially *precentral-SMA* coupling) signals later benefit and can guide adaptation (e.g., intensifying goal-directed, movement-linked practice blocks or pivoting components). Embedding such rules in adaptive trials can align practice dose and content to phase-specific target engagement, while a clinician-guided format safeguards safety in higher-risk settings.

The moderate AMN–SEC and PDR association in the rehabilitation arm is interpretable: manual, goal-directed activities plausibly strengthen sensorimotor–executive couplings and yield modest symptomatic improvement. What appears distinctive under meditation is the sequence: an early involvement of default-mode–cerebellar component followed by later action-mode executive engagement that tracks long-term clinical benefit, and such pattern is not evident with rehabilitation alone.

Our small cohort comprised only Asian male inpatients, which limits its generalizability. The cross-lagged path model and structural equation models support temporal precedence, which are still predictions rather than causality[34]. The imaging preprocessing, components derivation, signal complexity and connectivity estimations are pipeline-sensitive (atlas choice, denoising, motion, and etc.)[35]. Predictive markers require out-of-sample validation with harmonized preprocessing, more open meditation trail datasets are necessary for further validations. As for the future research, pre-registered phase-specific randomized controlled trails are needed to validate the biphasic model: early DMN–cerebellar down-weighting and later AMN–precentral/SMA engagement. Stratification and adaptation can use baseline DMN–cerebellar features and early AMN–SEC changes to guide continuation/augmentation of clinical meditation practice. Causal probes of

cerebellar and pre-SMA (e.g., non-invasive neuromodulation) are crucial to test whether nudging these circuits amplifies the corresponding phase of recovery.

In conclusion, the clinical trajectory and imaging markers suggest that daily clinician-guided meditation plus rehabilitation supports recovery via a biphasic brain network reconfiguration: the early default-mode–cerebellar involvement followed by later action-mode engagement, and provide phase-specific, information-based biomarkers (CCI, FC) for personalized deployment in schizophrenia and, potentially, other conditions characterized by imbalance between internally and externally oriented functionalities.

Methods and Materials

Study design and participants

We conducted an eight-month, parallel-group randomized clinical trial (registration ChiCTR1800014913) in male Han Chinese inpatients with schizophrenia and persistent positive symptoms. Eligible participants met DSM-IV criteria for schizophrenia, had illness duration ⩾ 5 years, and showed persistent hallucinations (PANSS P3 ⩾ 5) and/or delusions (⩾ 2 among P1/P5/P6/G1/G3/G9 ⩾ 5) despite ⩾ 2 adequate antipsychotic trials. Exclusion criteria included: any other major Axis I disorder; MMSE < 24; language barriers precluding consent/assessment; known neurological disease; major medical illness; and substance abuse or dependence. Participants were randomized 1:1 to clinician-guided meditation plus rehabilitation or rehabilitation alone. All participants completed 4 months; 63/64 completed 8 months (one control participant died of cardiac arrest, adjudicated unrelated to study procedures). Antipsychotic regimens were maintained under physician direction; doses were recorded and converted to chlorpromazine equivalents (CPZ). The trial adhered to the Declaration of Helsinki; written informed consent was obtained at enrolment. CONSORT flow and primary clinical outcomes have been reported previously[13].

Procedures

Interventions ran Monday–Sunday over the 8 months. The control arm received a 90-min general rehabilitation program (GRP) Monday–Saturday (manual work, gardening, painting, reading) plus a 90-min Sunday group intervention session (GIS) focused on daily-living skills and psychoeducation regarding schizophrenia, including self-acceptance. The meditation arm received 30 min clinician-guided meditation + 60 min GRP Monday–Saturday. Meditation comprised: (i) seven-point posture of Buddha Vairocana; (ii) abdominal breathing; (iii) sustained awareness of, and concentration on, the breath; and (iv) non-reactive attention to thoughts. The Sunday GIS for the meditation arm included (i) instruction in meditation methods and cultural context, (ii) psychoeducation regarding schizophrenia and self-acceptance, (iii) a 30-min practice, and (iv) group discussion of experiences and challenges. GISs were weekly for the first 8 weeks, then monthly. Clinical assessments and MRI were acquired at baseline, 3 months, and 8 months. All participants continued physician-directed antipsychotics throughout.

Demographics and clinical assessments

Baseline demographics (age, education, family income, smoking, age at onset, illness duration, current medications) were collected via structured questionnaire. Symptoms were assessed with the Positive and Negative Syndrome Scale (PANSS)[36]. The primary clinical outcome was the PANSS total Decrease Rate (PDR) with established rescaling[37]:

$$PDR_t = \frac{PANSS_0 - PANSS_t}{PANSS_0 - 30} \times 100\%$$

The PANSS subscale decrease rates were defined in the similar fashion and rescaling, rescale factors were 7, 7 and 16 for PANSS positive Decrease Rate (PPDR), PANSS negative Decrease Rate (PNDR) and PANSS general Decrease Rate (PGDR). Cognition was assessed with the Repeatable Battery for the Assessment of Neuropsychological Status (RBANS)[38], summarized as the RBANS Increase Rate (RIR) computed analogously but without rescaling. Mindfulness was assessed with the Five Facet Mindfulness Questionnaire (FFMQ)[39]. Antipsychotic exposure was indexed by chlorpromazine equivalents (CPZ). Full scoring details were summarized in Tab. S1-S2 of the supplementary materials.

Estimation of treatment effects

We estimated the average treatment effects (ATE) for PDR and RIR using linear mixed-effects models (LMM) with fixed effects for group (meditation vs GRP), session (baseline, 3 months, 8 months), and group×session, and subject-level random slopes to model within-participant correlation[40]. Models were fit by REML (statsmodels 0.14.4); we report model-based marginal mean differences with 95% confidence intervals and exact *p*-values To probe effect modification, baseline covariates (CPZ, RBANS, PANSS, FFMQ) entered group×covariate interactions to estimate conditional ATEs (CATEs); specifications and contrasts are detailed in the supplementary materials.

Temporal ordering between cognition and symptoms was examined with a cross-lagged panel model (CLPM) comprising autoregressive paths for PDR and RIR, direct treatment-to-outcome paths at each session, and cross-lags between PDR and RIR (semopy 2.3.11). We further performed bootstrap-based mediation analysis (10,000 resamples) to test indirect effects of treatment on 8-month PDR via 3-month RIR.

Identification of heterogeneous clinical trajectories

To characterize treatment-response heterogeneity, we fit latent-class linear mixed models (LCLMM) to PDR across sessions, considering 2–5 classes and selecting the most parsimonious model by BIC[30]. We summarized baseline profiles of classes using standardized mean differences (SMDs). Correlates of high-responder membership were examined with elastic-net logistic regression (5-fold cross-validation; 10,000 permutations) to obtain confidence intervals and *p*-values for the selected features[41].

Imaging acquisition and preprocessing

MRI data were acquired on a Siemens 3.0 T Verio with a 32-channel head coil. T1-weighted MPRAGE: matrix 256 × 256 × 224, voxel size 1 × 1 × 1 mm³, TR = 2530 ms, TE = 3.65 ms. Resting-state fMRI (rs-fMRI): gradient-echo EPI, matrix 74 × 74 × 51, voxel size 3 × 3 × 3 mm³, TR = 1500 ms, TE = 30 ms, flip angle 77°, duration 6 min (240 time points); the first 10 volumes were discarded. Data were converted to BIDS[42] with HeuDiConv v0.9.0[43], and preprocessed using fMRIPrep v22.1.1[44]. Preprocessed rs-fMRI were detrended and smoothed with a 6 mm FWHM Gaussian kernel (nilearn v0.10.4) [45]. To mitigate confounds, we regressed six motion parameters (three translational, three rotational) and the global signal according to literature recommendations[46]. Imaging quality control yielded 186 usable rs-fMRI images across sessions. Additional details are provided in the supplementary materials.

Functional components and temporal complexities

Large-scale activity patterns were estimated with group canonical ICA (canICA; k = 20 components) on all quality-controlled rs-fMRI data[31]. We binarized component maps and extracted mean time series per participant and session. For each component we computed two complementary temporal-complexity measures: sample entropy (SampEn) and the Hurst exponent (HE)[19,47,48]. SampEn quantifies signal irregularity (higher values indicate greater unpredictability). HE indexes long-range temporal dependence (HE > 0.5 indicates persistent dynamics) and typically changes towards 0.5 with increased signal complexity[49,50]. Components whose complexity predicted PDR were screened using elastic-net with 5-fold cross-validation and 10,000 permutations. To better assess the correlation between component signal complexity and PDR, we created a composed complexity index (*CCI*) that combined the two measures based on weighted *z*-scores, it can be expressed as:

$$CCI_{itc} = \frac{Z(SampEn_{itc}) + (1 - 2 \cdot \mathbf{1}\{HE_{itc} > 0.5\} \cdot Z(HE_{itc}))}{2},$$

where $\mathbf{1}\{HE_{itc} > 0.5\}$ is an indicator function that is 1 when HE_{itc} is larger than 0.5 otherwise 0, larger CCI_{itc} indicates higher overall signal complexity for component *c* at session *t* for subject *i*. We further tested phase-specific temporal precedence from component complexities to clinical improvement using a two-wave lagged structural equation model (SEM) (lavaan 0.6-18). Outcomes were PDR at 3 and 8 months. The model included: (i) autoregression for each component, (ii) two imaging to clinical paths: baseline DMN–CIC and AMN–SEC to 3-month PDR and 3-month DMN–CIC and AMN–SEC to 8-month PDR (treatment and carry over effects of meditation were also modeled), these two paths for subject *i* can be expressed as:

$PDR_{i3} \sim group_i + CCI_{i0(DMN-CIC)} + CCI_{i0(AMN-SEC)} + age_i + PANSS_{i0} + RBANS_{i0} + \varepsilon_{i3}$;

$PDR_{i8} \sim group_i + CCI_{i3(DMN-CIC)} + CCI_{i3(AMN-SEC)} + age_i + PANSS_{i0} + PDR_{i3} + \varepsilon_{i8}$; and

(iii) adjustments for age, baseline PANSS and RBANS. Within-wave covariances were freely estimated. We report the two focal path estimates with 95% CIs; full specification, additional paths, fit indices, and Wald tests are detailed in the supplementary materials.

Functional connectivity and predictive modeling

Functional connectivity (FC) was defined as the Pearson correlation between the time series from the regions of interest (ROI) defined by AAL2 atlas[51,52]. We evaluated three prediction tasks for each arm: (1) 3-month PDR from baseline FC; (2) 8-month PDR from baseline FC; (3) 8-month PDR from FC changes in the first 3 months (ΔFC_{3-0}). Models used z-scored FC values and elastic net with 5-fold cross-validated hyperparameters and 10,000 permutations to derive signed importance scores (magnitude=R^2 contributions; sign=direction of association with PDR)[32]. Edges with importance > 0.05 are listed as candidate predictors; full edgewise results are provided in the supplementary materials.

Software packages

All the above analyses used Python 3.9.12 and R 4.2.2 environments. Key packages include: *statsmodels* 0.14.4 (LMM), *semopy* 2.3.11 (CLPM), *HeuDiConv* 0.9.0, *fMRIPrep* 22.1.1, *nilearn* 0.10.4, lavaan 0.6-18 (SEM) and *lcmm* 2.1.0 (LCLMM).

Data availability

The data for statistical analysis and figures are shared together with the codes via GitHub: https://github.com/Vincent-wq/repo_sz_meditation. The data that support the findings of this study are available from the corresponding authors on reasonable request.

Code availability

The full analysis codes are shared via GitHub: https://github.com/Vincent-wq/repo_sz_meditation.

Acknowledgement

The authors would like to thank all the participants, doctors, nurses and students who were involved in the implementation of this RCT. The authors also would like to thank Dr. Pedro Antonio Valdés-Sosa and Dr. María Luisa Bringas-Vega for their feedbacks and insights in improve this manuscript. The authors thank Dr. Hu Chuan-Peng for his suggestions during the 2025 COSN hackathon.

Conflict of interests

All the co-authors declare no conflict of interests.

Funding

This research was supported by the National Key R&D Program of China (No. 2017YFC0909200); the Shanghai Mental Health Center Key Project (No. 23zd01), Shanghai Jiao Tong University Joint Art and Science Funding (No. 14JCRZ05); Shanghai Jiao Tong University Medical and Engineering Joint Grant (No. YG2016ZD06); Shanghai Key Laboratory of Psychotic Disorders Open Grant (No. 17-K04), and the Integrated Innovation Research Team of Shanghai Mental Health Center.

References

402 1. Goyal, M. *et al.* Meditation Programs for Psychological Stress and Well-being: A Systematic
403 Review and Meta-analysis. *JAMA Intern. Med.* **174**, 357–368 (2014).
404 2. Sparacio, A. *et al.* Self-administered mindfulness interventions reduce stress in a large,
405 randomized controlled multi-site study. *Nat. Hum. Behav.* 1–10 (2024) doi:10.1038/s41562-
406 024-01907-7.
407 3. van Agteren, J. *et al.* A systematic review and meta-analysis of psychological interventions to
408 improve mental wellbeing. *Nat. Hum. Behav.* **5**, 631–652 (2021).
409 4. Tang, Y.-Y., Hölzel, B. K. & Posner, M. I. The neuroscience of mindfulness meditation. *Nat.*
410 *Rev. Neurosci.* **16**, 213–225 (2015).
411 5. Mindfulness research needs an intervention. *Nat. Ment. Health* **1**, 437–438 (2023).
412 6. Kwok, J. Y. Y. *et al.* Effects of Mindfulness Yoga vs Stretching and Resistance Training
413 Exercises on Anxiety and Depression for People With Parkinson Disease: A Randomized
414 Clinical Trial. *JAMA Neurol.* **76**, 755–763 (2019).
415 7. Kwok, J. Y. Y. *et al.* A randomized clinical trial of mindfulness meditation versus exercise in
416 Parkinson's disease during social unrest. *Npj Park. Dis.* **9**, 7 (2023).
417 8. Cherkin, D. C. *et al.* Effect of Mindfulness-Based Stress Reduction vs Cognitive Behavioral
418 Therapy or Usual Care on Back Pain and Functional Limitations in Adults With Chronic Low
419 Back Pain: A Randomized Clinical Trial. *JAMA* **315**, 1240–1249 (2016).
420 9. Wells, R. E. *et al.* Effectiveness of Mindfulness Meditation vs Headache Education for Adults
421 With Migraine: A Randomized Clinical Trial. *JAMA Intern. Med.* **181**, 317–328 (2021).
422 10. Kuyken, W. *et al.* Efficacy of Mindfulness-Based Cognitive Therapy in Prevention of
423 Depressive Relapse: An Individual Patient Data Meta-analysis From Randomized Trials.
424 *JAMA Psychiatry* **73**, 565–574 (2016).
425 11. Polusny, M. A. *et al.* Mindfulness-Based Stress Reduction for Posttraumatic Stress Disorder
426 Among Veterans: A Randomized Clinical Trial. *JAMA* **314**, 456–465 (2015).

12. Liu, Y.-C., Li, I.-L. & Hsiao, F.-H. Effectiveness of mindfulness-based intervention on psychotic symptoms for patients with schizophrenia: A meta-analysis of randomized controlled trials. *J. Adv. Nurs.* **77**, 2565–2580 (2021).
13. Xue, T. *et al.* Eight-month intensive meditation-based intervention improves refractory hallucinations and delusions and quality of life in male inpatients with schizophrenia: a randomized controlled trial. *Psychiatry Clin. Neurosci.* **78**, 248–258 (2024).
14. Garrison, K. A., Zeffiro, T. A., Scheinost, D., Constable, R. T. & Brewer, J. A. Meditation leads to reduced default mode network activity beyond an active task. *Cogn. Affect. Behav. Neurosci.* **15**, 712–720 (2015).
15. Taren, A. A. *et al.* Mindfulness Meditation Training and Executive Control Network Resting State Functional Connectivity: A Randomized Controlled Trial. *Biopsychosoc. Sci. Med.* **79**, 674 (2017).
16. Cotier, F. A., Zhang, R. & Lee, T. M. C. A longitudinal study of the effect of short-term meditation training on functional network organization of the aging brain. *Sci. Rep.* **7**, 598 (2017).
17. Kajimura, S., Masuda, N., Lau, J. K. L. & Murayama, K. Focused attention meditation changes the boundary and configuration of functional networks in the brain. *Sci. Rep.* **10**, 18426 (2020).
18. Bremer, B. Mindfulness meditation increases default mode, salience, and central executive network connectivity. *Sci. Rep.* (2022).
19. He, B. J. Scale-Free Properties of the Functional Magnetic Resonance Imaging Signal during Rest and Task. *J. Neurosci.* **31**, 13786–13795 (2011).
20. Sokunbi, M. O. *et al.* Nonlinear Complexity Analysis of Brain fMRI Signals in Schizophrenia. *PLOS ONE* **9**, e95146 (2014).
21. Richman, J. S. & Moorman, J. R. Physiological time-series analysis using approximate entropy and sample entropy. *Am. J. Physiol.-Heart Circ. Physiol.* **278**, H2039–H2049 (2000).

452 22. Riegner, G., Dean, J., Wager, T. D. & Zeidan, F. Mindfulness Meditation and Placebo
453 Modulate Distinct Multivariate Neural Signatures to Reduce Pain. *Biol. Psychiatry* **97**, 81–88
454 (2025).
455 23. Thomas Yeo, B. T. *et al.* The organization of the human cerebral cortex estimated by intrinsic
456 functional connectivity. *J. Neurophysiol.* **106**, 1125–1165 (2011).
457 24. Buckner, R. L., Krienen, F. M., Castellanos, A., Diaz, J. C. & Yeo, B. T. T. The organization
458 of the human cerebellum estimated by intrinsic functional connectivity. *J. Neurophysiol.* **106**,
459 2322–2345 (2011).
460 25. Guell, X., Schmahmann, J. D., Gabrieli, J. D. & Ghosh, S. S. Functional gradients of the
461 cerebellum. *eLife* **7**, e36652 (2018).
462 26. Menon, V. 20 years of the default mode network: A review and synthesis. *Neuron* **111**, 2469–
463 2487 (2023).
464 27. Dosenbach, N. U. F., Raichle, M. E. & Gordon, E. M. The brain's action-mode network. *Nat.*
465 *Rev. Neurosci.* **26**, 158–168 (2025).
466 28. Ariani, G., Shahbazi, M. & Diedrichsen, J. Cortical Areas for Planning Sequences before and
467 during Movement. *J. Neurosci.* **45**, e1300242024 (2025).
468 29. Nguyen, K. P. & Person, A. L. Cerebellar circuit computations for predictive motor control.
469 *Nat. Rev. Neurosci.* **26**, 538–553 (2025).
470 30. Proust-Lima, C., Philipps, V. & Liquet, B. Estimation of Extended Mixed Models Using
471 Latent Classes and Latent Processes: The *R* Package **lcmm**. *J. Stat. Softw.* **78**, (2017).
472 31. Varoquaux, G. *et al.* A group model for stable multi-subject ICA on fMRI datasets.
473 *NeuroImage* **51**, 288–299 (2010).
474 32. Breiman, L. Random Forests. *Mach. Learn.* **45**, 5–32 (2001).
475 33. Li, M., Sun, H., Huang, Y. & Chen, H. Shapley value: from cooperative game to explainable
476 artificial intelligence. *Auton. Intell. Syst.* **4**, 2 (2024).
477 34. Wang, Q., Wang, Q. & Zhang, R.-Y. Claim causality with clarity. *Psychoradiology* **3**, kkad007
478 (2023).

35. Wang, Q. *et al.* Reproducibility of cerebellar involvement as quantified by consensus structural MRI biomarkers in advanced essential tremor. *Sci. Rep.* **13**, 581 (2023).
36. Kay, S. R., Fiszbein, A. & Opler, L. A. The Positive and Negative Syndrome Scale (PANSS) for Schizophrenia. *Schizophr. Bull.* **13**, 261–276 (1987).
37. Obermeier, M. *et al.* Should the PANSS Be Rescaled? *Schizophr. Bull.* **36**, 455–460 (2010).
38. Randolph, C., Tierney, M. C., Mohr, E. & Chase, T. N. The Repeatable Battery for the Assessment of Neuropsychological Status (RBANS): Preliminary Clinical Validity. *J. Clin. Exp. Neuropsychol.* **20**, 310–319 (1998).
39. Baer, R. A. *et al.* Construct Validity of the Five Facet Mindfulness Questionnaire in Meditating and Nonmeditating Samples. *Assessment* **15**, 329–342 (2008).
40. Hernán, M. A. & Robins, J. M. *Causal Inference: What If.* (Boca Raton: Chapman & Hall/CRC, 2020).
41. Zou, H. & Hastie, T. Regularization and Variable Selection Via the Elastic Net. *J. R. Stat. Soc. Ser. B Stat. Methodol.* **67**, 301–320 (2005).
42. Gorgolewski, K. J. *et al.* The brain imaging data structure, a format for organizing and describing outputs of neuroimaging experiments. *Sci. Data* **3**, 160044 (2016).
43. Halchenko, Y. *et al.* nipy/heudiconv v0.9.0. Zenodo https://doi.org/10.5281/zenodo.4390433 (2020).
44. Esteban, O. *et al.* fMRIPrep: a robust preprocessing pipeline for functional MRI. *Nat. Methods* **16**, 111–116 (2019).
45. contributors, N. *et al.* nilearn. Zenodo https://doi.org/10.5281/zenodo.10579570 (2024).
46. Fox, M. D. *et al.* The human brain is intrinsically organized into dynamic, anticorrelated functional networks. *Proc. Natl. Acad. Sci.* **102**, 9673–9678 (2005).
47. Martínez Vivot, R., Pallavicini, C., Zamberlan, F., Vigo, D. & Tagliazucchi, E. Meditation Increases the Entropy of Brain Oscillatory Activity. *Neuroscience* **431**, 40–51 (2020).
48. Shen, K., McFadden, A. & McIntosh, A. R. Signal complexity indicators of health status in clinical EEG. *Sci. Rep.* **11**, 20192 (2021).

49. Dong, J. *et al.* Hurst Exponent Analysis of Resting-State fMRI Signal Complexity across the Adult Lifespan. *Front. Neurosci.* **12**, (2018).

50. Linke, A. C. *et al.* Altered Development of the Hurst Exponent in the Medial Prefrontal Cortex in Preschoolers With Autism. *Biol. Psychiatry Cogn. Neurosci. Neuroimaging* S2451902224002714 (2024) doi:10.1016/j.bpsc.2024.09.003.

51. Friston, K. J. Functional and Effective Connectivity: A Review. *Brain Connect.* **1**, 13–36 (2011).

52. Rolls, E. T., Joliot, M. & Tzourio-Mazoyer, N. Implementation of a new parcellation of the orbitofrontal cortex in the automated anatomical labeling atlas. *NeuroImage* **122**, 1–5 (2015).

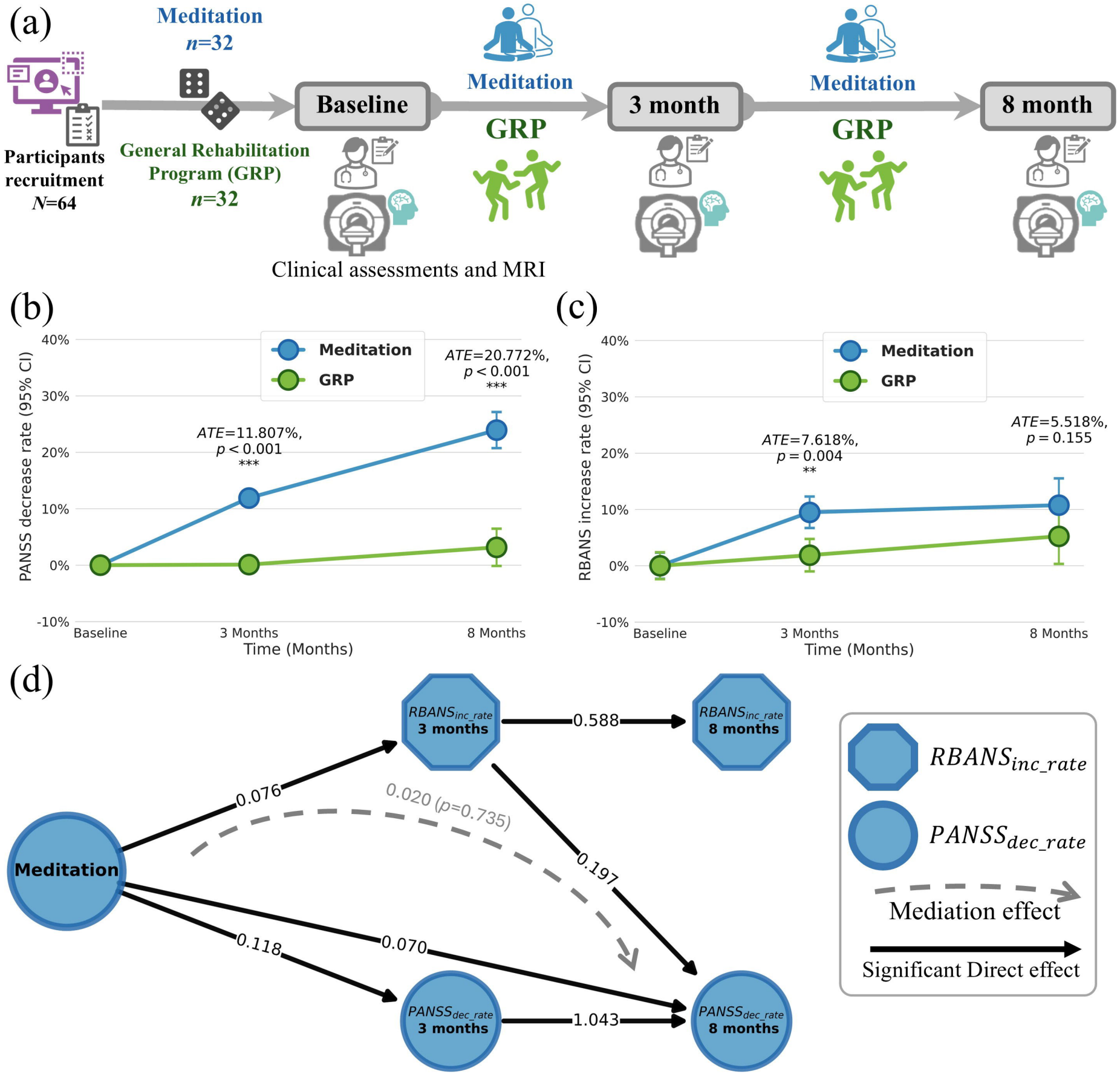
(a)
Meditation
n=32
Participants recruitment
N=64
General Rehabilitation Program (GRP)
n=32
Baseline
Meditation
GRP
3 month
Meditation
GRP
8 month
Clinical assessments and MRI
(b)
Meditation
GRP
ATE=20.772%, p < 0.001 ***
ATE=11.807%, p < 0.001 ***
PANSS decrease rate (95% CI)
40%
30%
20%
10%
0%
-10%
Baseline
3 Months
8 Months
Time (Months)
(c)
Meditation
GRP
ATE=5.518%, p = 0.155
ATE=7.618%, p = 0.004 **
RBANS increase rate (95% CI)
40%
30%
20%
10%
0%
-10%
Baseline
3 Months
8 Months
Time (Months)
(d)
RBANSinc_rate 3 months
RBANSinc_rate 8 months
0.588
0.076
0.020 (p=0.735)
0.197
Meditation
0.118
0.070
PANSSdec_rate 3 months
1.043
PANSSdec_rate 8 months
RBANSinc_rate
PANSSdec_rate
Mediation effect
Significant Direct effect

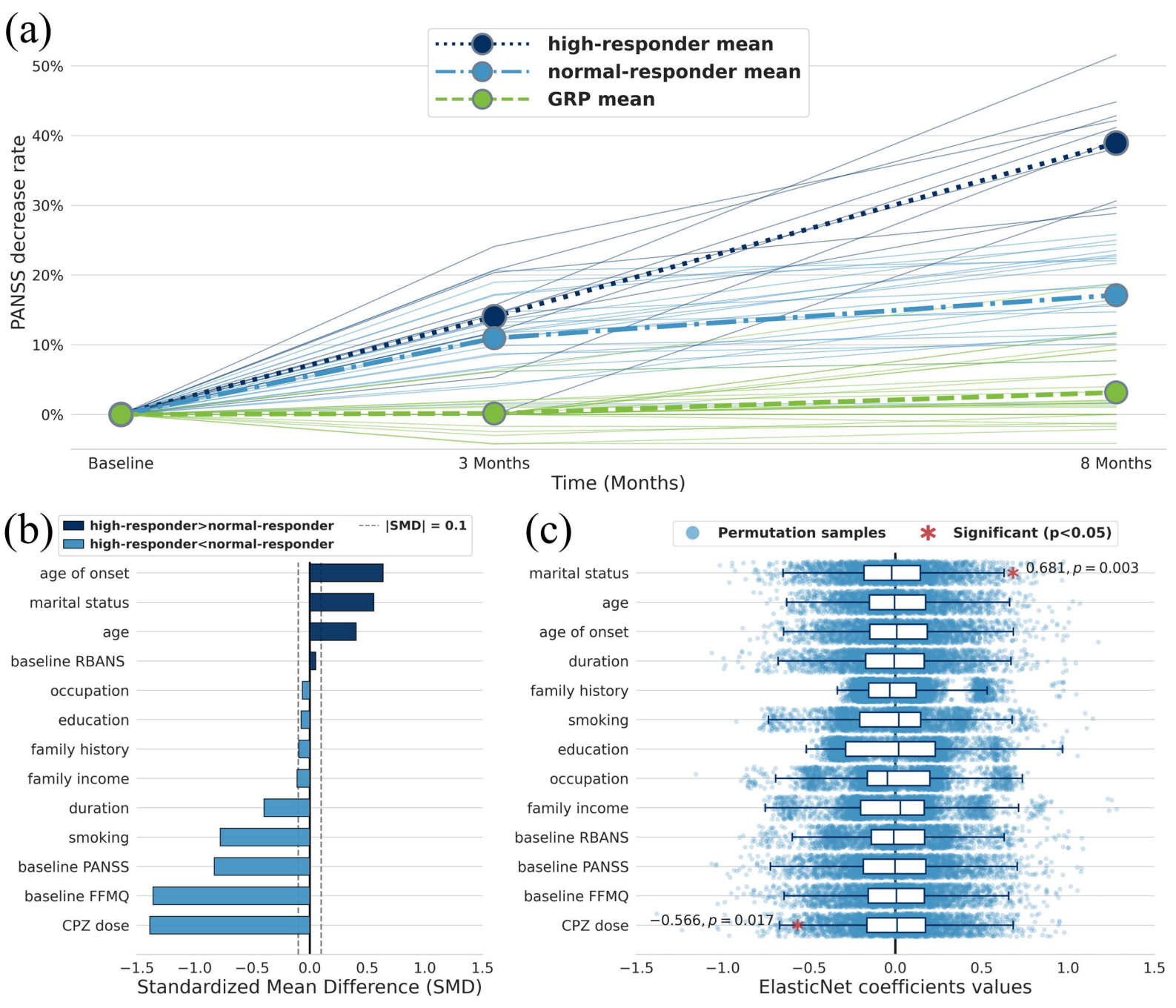
(a)
high-responder mean
normal-responder mean
GRP mean
PANSS decrease rate
50%
40%
30%
20%
10%
0%
Baseline
3 Months
8 Months
Time (Months)
(b)
high-responder>normal-responder
high-responder<normal-responder
|SMD| = 0.1
age of onset
marital status
age
baseline RBANS
occupation
education
family history
family income
duration
smoking
baseline PANSS
baseline FFMQ
CPZ dose
−1.5
−1.0
−0.5
0.0
0.5
1.0
1.5
Standardized Mean Difference (SMD)
(c)
Permutation samples
Significant (p<0.05)
0.681, p = 0.003
−0.566, p = 0.017
marital status
age
age of onset
duration
family history
smoking
education
occupation
family income
baseline RBANS
baseline PANSS
baseline FFMQ
CPZ dose
−1.5
−1.0
−0.5
0.0
0.5
1.0
1.5
ElasticNet coefficients values

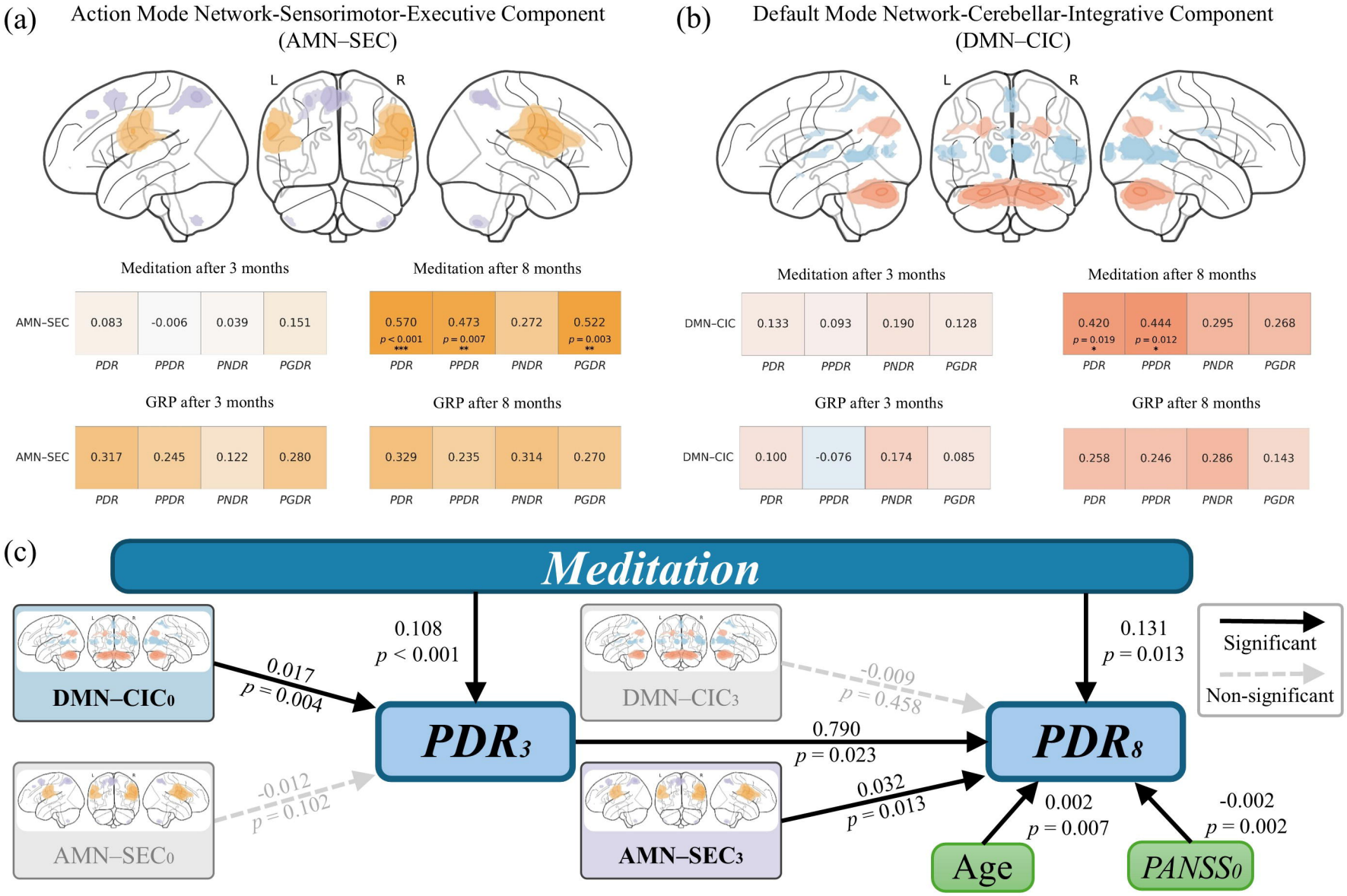
(a)
Action Mode Network-Sensorimotor-Executive Component (AMN–SEC)
L
R
Meditation after 3 months
AMN-SEC 0.083 -0.006 0.039 0.151
PDR PPDR PNDR PGDR
Meditation after 8 months
0.570 p < 0.001 *** 0.473 p = 0.007 ** 0.272 0.522 p = 0.003 **
PDR PPDR PNDR PGDR
GRP after 3 months
AMN-SEC 0.317 0.245 0.122 0.280
PDR PPDR PNDR PGDR
GRP after 8 months
0.329 0.235 0.314 0.270
PDR PPDR PNDR PGDR
(b)
Default Mode Network-Cerebellar-Integrative Component (DMN–CIC)
L
R
Meditation after 3 months
DMN-CIC 0.133 0.093 0.190 0.128
PDR PPDR PNDR PGDR
Meditation after 8 months
0.420 p = 0.019 * 0.444 p = 0.012 * 0.295 0.268
PDR PPDR PNDR PGDR
GRP after 3 months
DMN-CIC 0.100 -0.076 0.174 0.085
PDR PPDR PNDR PGDR
GRP after 8 months
0.258 0.246 0.286 0.143
PDR PPDR PNDR PGDR
(c)
Meditation
DMN–CIC0
0.017 p = 0.004
0.108 p < 0.001
DMN–CIC3
-0.009 p = 0.458
0.131 p = 0.013
Significant
Non-significant
PDR3
0.790 p = 0.023
PDR8
AMN–SEC0
-0.012 p = 0.102
AMN–SEC3
0.032 p = 0.013
0.002 p = 0.007
-0.002 p = 0.002
Age
PANSS0

(a) Predicting 3-month PDR using baseline FC

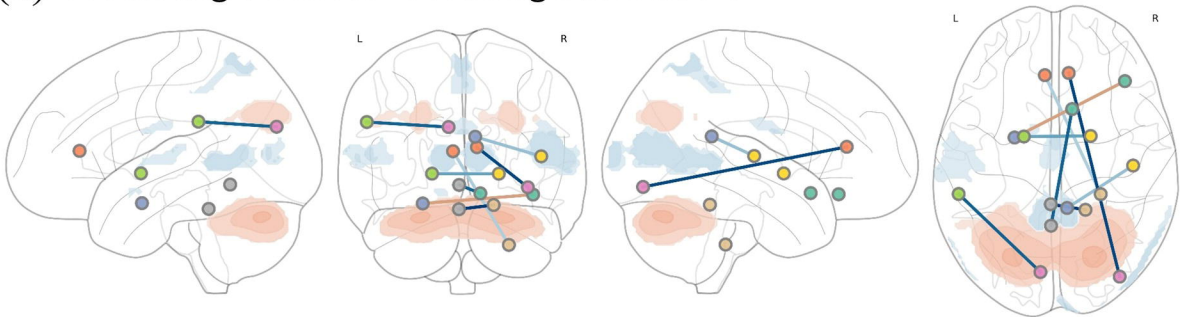

FC pairs	Signed Importance	Std.
Cerebelum_4_5_R - Vermis_1_2	-0.119	0.035
Cingulum_Ant_R - Occipital_Inf_R	-0.110	0.033
Olfactory_R - Vermis_4_5	-0.091	0.028
Cuneus_L - SupraMarginal_L	-0.091	0.030
Pallidum_L - Pallidum_R	-0.054	0.018

(b) Predicting 8-month PDR using baseline FC

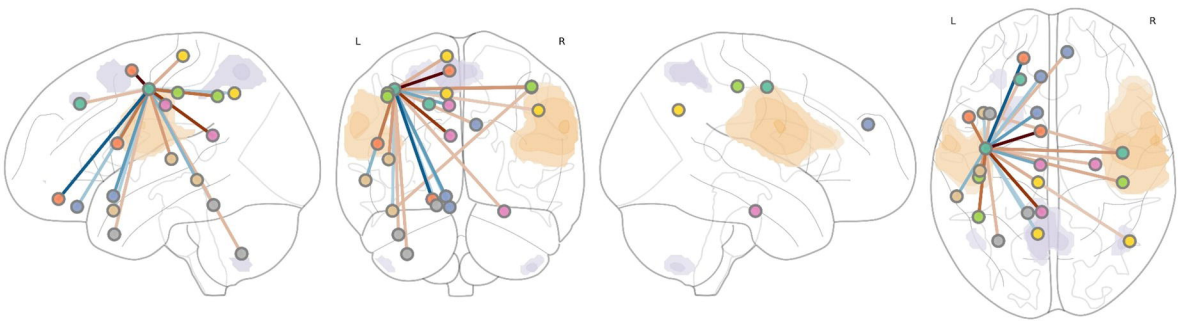

FC pairs	Signed Importance	Std.
Precentral_L - Supp_Motor_Area_L	0.154	0.028
Precentral_L - Cingulum_Post_L	0.110	0.020
Precentral_L - Frontal_Sup_Orb_L	-0.095	0.018
Precentral_L - Parietal_Inf_L	0.078	0.014
Precentral_L - Frontal_Inf_Oper_L	0.069	0.013
Precentral_L - Olfactory_L	-0.058	0.011
Precentral_L - Precentral_R	0.052	0.010
Precentral_L - Cingulum_Mid_L	-0.052	0.009

(c) Predicting 8-month PDR using FC changes between 3-month and baseline

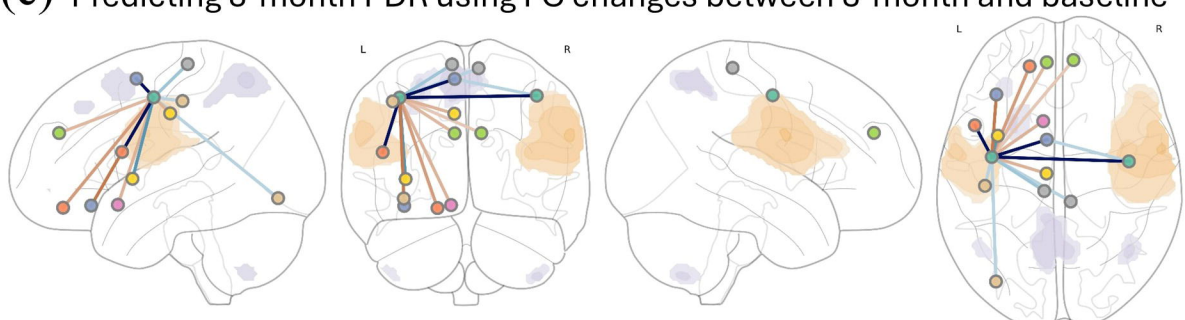

FC pairs	Signed Importance	Std.
Precentral_L - Supp_Motor_Area_L	-0.371	0.067
Precentral_L - Frontal_Inf_Oper_L	-0.322	0.059
Precentral_L - Precentral_R	-0.253	0.046
Precentral_L - Frontal_Inf_Orb_L	0.070	0.013
Precentral_L - Insula_L	-0.062	0.011
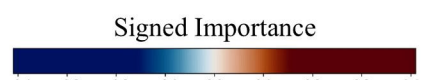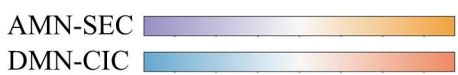
(Importance>0.05)